Macromolecules
ARTICLE

Macromolecules **2010**, *43*, 2721–2731 **2721**
DOI: 10.1021/ma9027257

Preparation of Hairy Particles and Antifouling Films Using Brush-Type Amphiphilic Block Copolymer Surfactants in Emulsion Polymerization

Alexandra Muñoz-Bonilla,[†,‡] Alex M. van Herk,[†] and Johan P. A. Heuts*[,†]

[†]*Laboratory of Polymer Chemistry, Eindhoven University of Technology, P.O. Box 513, 5600 MB Eindhoven, The Netherlands, and* [‡]*Instituto de Ciencia y Tecnología de Polímeros (CSIC), C/Juan de la Cierva 3, 28006 Madrid, Spain*

Received December 10, 2009; Revised Manuscript Received February 11, 2010

ABSTRACT: Two series of well-defined brush-type amphiphilic block copolymers of polystyrene-*b*-poly[poly(ethylene glycol) methyl ether methacrylate] (PS-*b*-P(PEGMA300) and PS-*b*-P(PEGMA1100)) were synthesized via atom transfer radical polymerization (ATRP) and used as surfactants in emulsion polymerization. The self-assembly behavior of these block copolymers in aqueous solution was studied by dynamic light scattering and cryogenic transmission electron microscopy. The critical micelle concentration of the synthesized polymers was found to depend on the length of the PEG side chains, but neither on the molar mass of the P(PEGMA) blocks nor the temperature. All of the block copolymers form micelles in the nanometer range. Emulsion polymerizations of styrene were carried out using the obtained brush-type amphiphilic block copolymers, and the influence of the block copolymer structure, surfactant concentration, and temperature was studied. The PS-*b*-P(PEGMA1100) copolymers seem to be the most efficient surfactants at low polymerization temperature, providing good colloidal stability. Monodisperse hairy particles with core−shell structures (observed by cryo-TEM) were obtained using the block copolymers with the long PEG side chain and the highest molar mass. Polystyrene films prepared from the latexes, containing the brush-type copolymers, display a lower contact angle than that obtained in films with conventional low molecular weight surfactants. In addition, the incorporation of PEGMA brushes on the polystyrene particles, and hence on the films, decreases the adsorption of proteins and, in this particular case, of bovine serum albumin.

Introduction

Well-defined polymer particles have aroused increasing interest in a broad variety of "high-tech" application areas such as optical data storage,[1] security data encryption,[2] photonic crystals,[3] and biotechnological or medical applications.[4,5] Furthermore, hairy polymer particles are particularly interesting due to their core−shell structure. One important property of the hairy particles is the possibility to include certain functionality on the shell periphery. Hairy particles are usually synthesized by "grafting from" or "grafting onto" processes.[6,7] As an alternative, these particles can also be prepared by using polymeric surfactants, mainly block and graft copolymers in an emulsion polymerization system.[8−13] Polymeric surfactants exhibit interesting properties in emulsion polymerization, such as their low critical micelle concentration, and because of their lower mobility, they have a much greater tendency to stay at the interface. The possibility of using hydrophilic blocks with high affinity to the aqueous medium and certain functionality together with their low diffusion coefficients allows the preparation of hairy particles with a shell composed of functional polymer chains. For instance, the use of block copolymers based on poly(ethylene glycol) (PEG) as stabilizers leads to the immobilization of antifouling polymer segments on the particle surface. PEG polymers are extensively employed in many biomedical applications due to their biocompatibility and protein-resistant properties.[14−17] Commonly, tissue culture polystyrene is used as substrate for cell cultures because of the numerous advantages of polystyrene such as its transparency, processability, sterizability, or low cost. A variety of methods has been studied in order to tailor the adhesion properties or to avoid the nonspecific adsorption of proteins.[18−20]

In this study antifouling polystyrene films were prepared from hairy particles synthesized using PEG-based brush-type amphiphilic block copolymers as stabilizers. Electrically neutral hydrophilic polymers such as PEG have shown to inhibit protein adsorption. Since the graft density of PEG chains and their block lengths are important for achieving high protein repellency, PEG-based comb polymer should have different antifouling properties than linear PEG polymers.[21−26] In this respect, several well-defined polystyrene-*b*-poly[poly(ethylene glycol) methyl ether methacrylate] (PS-*b*-P(PEGMA)) copolymers were synthesized via atom transfer radical polymerization (ATRP), varying the number of repeating PEGMA units of the hydrophilic blocks and also the number of ethylene glycol units of the side chains.

It is well-known that amphiphilic block copolymers can self-assemble in a selective solvent into a variety of morphologies, such as micelles, vesicles, or cylinders, depending on their chemical composition, molecular weight, and architecture.[27−29] However, relatively few studies have been previously published regarding the aggregation into micelles of brush-type amphiphilic block copolymers based on P(PEGMA).[30−39] In this article we study in more detail the solution behavior and the self-assembly into micelles of the synthesized block copolymers. In the majority of the research on nonionic polymeric surfactants, block copolymers based on linear poly(ethylene glycol) are typically used. A few studies have been reported using PEGMA macromonomer as reactive surfactant[40−44] and amphiphilic graft copolymers consisting of monomeric units of PEG acrylate.[45] However, to the best of our knowledge, no work has been published on emulsion polymerization using brush-type amphiphilic block

*Corresponding author. E-mail: j.p.a.heuts@tue.nl.

Published on Web 02/19/2010

copolymers based on P(PEGMA) as the polymeric surfactant. The purpose of this work is to evaluate the surfactant efficiency of the different brush-type amphiphilic copolymers in emulsion polymerization and whether they impart fouling resistance properties to polystyrene films.

Experimental Section

Materials. Poly(ethylene glycol) methyl ether methacrylate (PEGMA300, $M_n \sim 300$ g mol^{-1}, Aldrich) and poly(ethylene glycol) methyl ether methacrylate (PEGMA1100, $M_n \sim 1100$ g mol^{-1}, Aldrich) were used as received. Styrene (99%, Aldrich) was purified by passing over a basic alumina column. Ethyl α-bromoisobutyrate (EBrIB) (97%+, Aldrich), copper(I) bromide (Cu(I)Br) (98%, Aldrich), copper(I) chloride (Cu(I)Cl) (99%, Aldrich), 2,2′-bipyridine (bpy) (99%+, Aldrich), *N*,*N*′,*N*″,*N*″′-pentamethyldiethylenetriamine (PMDETA) (99%, Aldrich), potassium persulfate (99%+, Aldrich), ammonium persulfate (98%+, Aldrich), and sodium thiosulfate (99%+, Sigma) were used as received. All organic solvents toluene, pentane, and tetrahydrofuran were AR grade and supplied by Biosolve. The dialysis tubing (with cutoff molecular weight of 3500) was purchased from Serva. Bovine albumin−fluorescein isothiocyanate conjugate was supplied by Sigma-Aldrich.

Synthesis of Polystyrene Macroinitiator via ATRP. In a typical experiment, styrene (10.000 g, 96 mmol), EBrIB (0.312 g, 1.6 mmol), and PMDETA (0.277 g, 1.6 mmol) were placed into a Schlenk tube. The solution was deoxygenated by at least three freeze−pump−thaw cycles, followed by the addition of Cu(I)Br (0.229 g, 1.6 mmol) under argon. Subsequently, another freeze−pump−thaw cycle was performed, and the reaction mixture was immersed into an oil bath at 85 °C and stirred under argon. After 4 h, the mixture was dissolved in THF and passed through an alumina column to remove the copper catalyst. The polymer was recovered after precipitation in methanol and dried under vacuum prior to SEC, NMR, and MALDI analyses.

Synthesis of Brush-Type Amphiphilic Block Copolymers of PS-*b*-P(PEGMA300). A typical synthesis was as follows: the polystyrene macroinitiator (0.490 g, 0.12 mmol) was dissolved in 4 mL of toluene in a Schlenk tube. PEGMA300 monomer (4.200 g, 14.0 mmol) and PMDETA (0.020 g, 0.12 mmol) were then added into the solution. The mixture was degassed by four freeze−pump−thaw cycles. After the addition of Cu(I)Cl (0.012 g, 0.12 mmol), one more freeze−pump−thaw cycle was performed. The polymerization was carried out at 90 °C under an argon atmosphere. After the desired time, the polymerization was stopped and the mixture passed over alumina column. The block copolymer was obtained by pouring the solution into pentane and drying the precipitate under vacuum.

Synthesis of Brush-Type Amphiphilic Block Copolymers of PS-*b*-P(PEGMA1100). PEGMA1100 was polymerized by ATRP from the polystyrene macroinitiator. All polymerizations were carried out as follows: a Schlenk tube containing PEGMA1100 monomer (7.700 g, 7.0 mmol), 10 mL of toluene, polystyrene macroinitiator (0.294 g, 0.07 mmol), and bpy (0.022 g, 0.14 mmol) was subjected to four freeze−pump−thaw cycles and one more after the addition of Cu(I)Br (0.010 g, 0.07 mmol). The mixture was heated at 90 °C under argon. At the desired time, the solution was diluted with THF and purified by passing it over an alumina column. The solutions were poured into pentane and the copolymers isolated. After that, the copolymers were dissolved in water and purified by dialysis to remove the residual monomer, and finally, the copolymers were obtained by freeze-drying.

Self-Assembly of the Brush-Type Amphiphilic Block Copolymers in Aqueous Solution. In a typical process, the micellar solution was prepared by dissolving the block copolymer in a few drops of THF, and subsequently pure water was added dropwise with vigorous stirring. The sample was transferred to dialysis tubing, sealed, and dialyzed against distilled water to remove the THF. The water surrounding the tubing was changed several times.

Emulsion Polymerization of Styrene with Brush-Type Block Copolymers as Stabilizers. All the emulsion polymerizations of styrene were carried out in batch, in a three-neck reactor with a reflux condenser, an argon inlet, and a mechanical stirrer. The recipes used for the preparation of the functional polystyrene particles are summarized in Table 3. In a typical recipe (Table 3, entry 6) the micellar solution (0.277 g of block copolymer in water) was prepared as described above. The micellar solution was transferred to the reactor, and the remainder of the water needed to reach a total of 36.600 g of water was added. The monomer styrene (8.300 g) was placed into the reactor, and the mixture was purged with argon for 30 min under stirring. The degassed solution was heated at 35 or 70 °C for the emulsion polymerization carried out using a redox or thermal initiator, respectively. The redox initiator solution (0.069 g of ammonium persulfate and 0.069 g of sodium thiosulfate in 5.000 g of water) or the thermal initiator solution (0.069 g of potassium persulfate in 5.000 g of water) was injected to start the polymerization. The argon flow was maintained throughout the reaction. At different reaction times, aliquots were extracted by syringe under an argon flow. A small amount of hydroquinone was added to these aliquots to quench the radical polymerization, and the monomer conversion was determined by gravimetry.

Measurements. ^{1}H NMR spectra were recorded on a Varian 400 MHz spectrometer using deuterated chloroform as solvent. SEC analyses were carried out on a Waters Alliance system equipped with a Waters 2695 separation module, a Waters 2414 refractive index detector (40 °C), and a Water 486 UV detector at 60 °C. DMF containing 0.05 M LiBr was used as eluent at a flow rate of 1 mL min^{-1}. The molecular weights were estimated against polystyrene standards. MALDI-ToF-MS analysis was carried out on a Voyager DE-STR from Applied Biosystems. The matrix used for the analysis was *trans*-2-[3-(4-*tert*-butylphenyl)-2-methyl-2-propenylidene]malononitrile (DCTB) and potassium trifluoracetate (Aldrich, 98%) as a cationization agent. For determining the lower critical solution temperature (LCST) a Hewlett-Packard 8453 spectrometer was used at 500 nm wavelength. The temperature was increased by 0.5 °C min^{-1}, and the cloud point was taken when the solution reached 50% of the maximum absorbance. The particle size distributions were determined by dynamic light scattering (DLS) using a Malvern Zetasizer Nano ZS instrument at 25 °C. Malvern Dispersion Software was used for data acquisition and analysis, applying the general purpose algorithm for calculating the size distribution. Critical micelle concentrations were determined from light scattering intensity measurements performed on a Malvern 4700 light scattering instrument (λ = 488 nm) equipped with a Malvern Multi-8 7032 correlator at a scattering angle of 90° at 25 and 65 °C. (Cryogenic) transmission electron microscopy (cryo-TEM and TEM) measurements were performed on a FEI Tecnai 20, type Sphera TEM instrument (with a LaB_6 filament, operating voltage = 200 kV). The particle size distributions were obtained from statistical treatment of representative TEM images for each sample using the software ImageJ. Average particle diameters and polydispersities were determined from these particle size distributions. For cryogenic measurements (cryo-TEM) the sample vitrification procedure was performed by using an automated vitrification robot (FEI Vitrobot Mark III). A 3 μL sample was applied to a Quantifoil grid (R 2/2, Quantifoil Micro Tools GmbH; freshly glow discharged for 40 s just prior to use) within the environmental chamber of the Vitrobot, and the excess liquid was blotted away. Afterward, the grid was rapidly plunged into liquid ethane at its melting temperature, resulting in a vitrified film. The grid containing vitrified film was immediately transferred to a cryo-holder (Gatan 626) and observed under low dose conditions at −170 °C. Scanning electron microscopy (SEM) micrographs

were taken using a JEOL JSM-5600 with an acceleration voltage of 10 kV. Latex particle films were gold-coated prior to scanning. Contact angles were measured with deionized water on a Dataphysics OCA 30 instrument at room temperature. Dynamic advancing and receding contact angles were recorded while water was added to and withdrawn from the drop, respectively, by a syringe pump. Nonspecific protein adsorption was determined using a steady-state fluorescence spectrometer (Edinburgh Instruments FS920). Emission spectra were recorded from 500 to 800 nm using excitation light of 490 nm.

Results and Discussion

Synthesis of Brush-Type Amphiphilic Block Copolymers. A series of PS-*b*-P(PEGMA300) and PS-*b*-P(PEGMA1100) block copolymers were prepared via ATRP in which the chemical compositions were varied. For the chain extension of the PS macroinitiator with PEGMA300 the use of CuCl instead of CuBr was required to obtain a good control of the polymerization. The length of the hydrophobic PS block was kept constant in all experiments (M_n = 4200 g mol^{-1}, 40 units) while the hydrophilic block of P(PEGMA300) (4.5 ethylene oxide units per monomer unit) or P(PEGMA1100) (22.7 ethylene oxide units per monomer unit) was varied. All SEC chromatograms showed a monomodal peak and narrow molecular weight distribution, indicating that the copolymers were obtained in a controlled manner (see Figure 1).

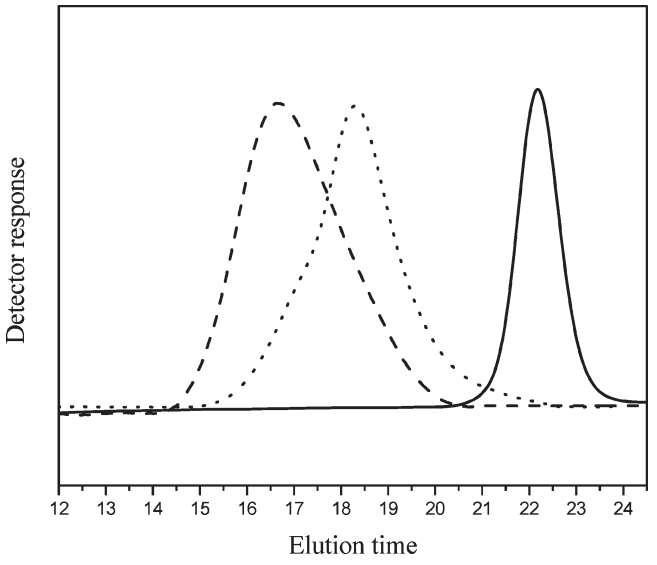

Figure 1. Size exclusion chromatograms recorded in DMF of chain extension polymerization by ATRP in toluene at 90 °C of (—) polystyrene macroinitiator (PS_{40}) with (···) poly[(ethylene glycol) methyl ether methacrylate (PEGMA300, $M_n \sim 300$ g mol^{-1}), yielding PS_{40}-*b*-$P(PEGMA300)_{54}$ diblock copolymer, and with (---) poly(ethylene glycol) methyl ether methacrylate (PEGMA1100, $M_n \sim 1100$ g mol^{-1}), yielding PS_{40}-*b*-$P(PEGMA1100)_{70}$.

The number-average molecular weights (M_n) and the polydispersity indices (M_w/M_n) of the corresponding block copolymers deduced from both SEC and ^{1}H NMR results and their estimated hydrophilic lypophilic balances (HLB) are listed in Table 1.

Additionally, several block copolymers of PS-*b*-P(PEGMA300) were prepared from the PS_{40} macroinitiator, using even higher PEGMA300 contents than those listed in Table 1 (degrees of polymerization higher than 100). However, broad molecular weight distributions, the appearance of a high and/or a low molecular weight shoulder, and, in some cases, gel formation were observed. This poor control can be attributed to the occurrence of chain coupling reactions and chain transfer to PEG moieties.[46−48] Several other attempts were also made to prepare these larger blocks using different experimental conditions (e.g., bpy/CuCl), but these led to similar results. Considering these results, we will only focus on the block copolymers with P(PEGMA300) blocks shorter than 100 units.

Aggregation Behavior of Brush-Type Amphiphilic Block Copolymers in Aqueous Solution. All of the synthesized amphiphilic block copolymers synthesized in this article were not directly soluble in water. Therefore, micelles were prepared by first dissolving a certain amount of block copolymer in THF, which is a cosolvent for both blocks. Deionized water was then added dropwise with vigorous stirring. Samples were transferred to dialysis tubing, sealed, and dialyzed against distilled water. The removal of the nonselective organic solvent by dialysis against water along with the high T_g of the PS core blocks result in frozen micelles as shown in previous studies.[49,50] Several copolymer concentrations were prepared by dilution of the most concentrated solution. The formation of micelles in aqueous solution was determined by measuring the scattering light intensity as a function of block copolymer concentration as shown in Figure 2. The polymer concentration at which the scattered intensity increases abruptly due to aggregate formation was used to estimate the critical micelle concentration (cmc) by the intersection of the two linear regression lines. As shown in Table 2 and in Figure 2, all of the PS-*b*-P(PEGMA1100) block copolymers with fixed poly(ethylene glycol) side chain show approximately the same cmc values, taking into account the uncertainties, ~0.2 mg mL^{-1}, suggesting that the cmc is not much affected by the length of the hydrophilic blocks (in the investigated molecular weight ranges). A similar behavior was found for the copolymers having short PEG side chain, PS-*b*-P(PEGMA300), which also display a value of cmc which is almost independent of the molar mass of the hydrophilic block. However, the cmc of these copolymers, around ~0.4 mg mL^{-1}, is much higher than that found

Table 1. Molecular Characteristics of the Polystyrene-*b*-poly[poly(ethylene glycol) methyl ether methacrylate] (PS-*b*-P(PEGMA300), PS-*b*-(PEGMA1100)) Block Copolymers and Their Precursor, Polystyrene Macroinitiator, Synthesized by ATRP

chemical structrure	$M_{n,SEC}$[a]	$M_{n,NMR}$[b]	M_w/M_n[a]	HLB_{ST}[d]	HLB_{MOD}[e]
PS_{40}	4 200	3 900[c]	1.09		
PS_{40}-*b*-$P(PEGMA300)_{60}$	20 200	22 200	1.22	16.2	10.8
PS_{40}-*b*-$P(PEGMA300)_{80}$	25 600	28 200	1.36	17.0	11.2
PS_{40}-*b*-$P(PEGMA300)_{87}$	32 100	30 300	1.27	17.2	11.4
PS_{40}-*b*-$P(PEGMA1100)_{30}$	33 000	37 200	1.34	17.7	16.1
PS_{40}-*b*-$P(PEGMA1100)_{54}$	58 000	63 600	1.27	18.7	17.0
PS_{40}-*b*-$P(PEGMA1100)_{70}$	58 800	81 200	1.52	19.0	17.2

[a] SEC analysis, DMF, PS standards. [b] Calculated from integral ratio of P(PEGMA):PS compared to PS macroinitiator M_n by SEC. [c] MALDI-ToF-MS. [d] The hydrophilic lypophilic balance calculated according to the Stöver method, HLB_{ST} = (wt % of hydrophilic portion)/5 (based on PEGMA content).[35] [e] The hydrophilic lypophilic balance according to our modified method, HLB_{MOD} = (wt % of hydrophilic portion)/5 (based on ethylene oxide content) (see text).

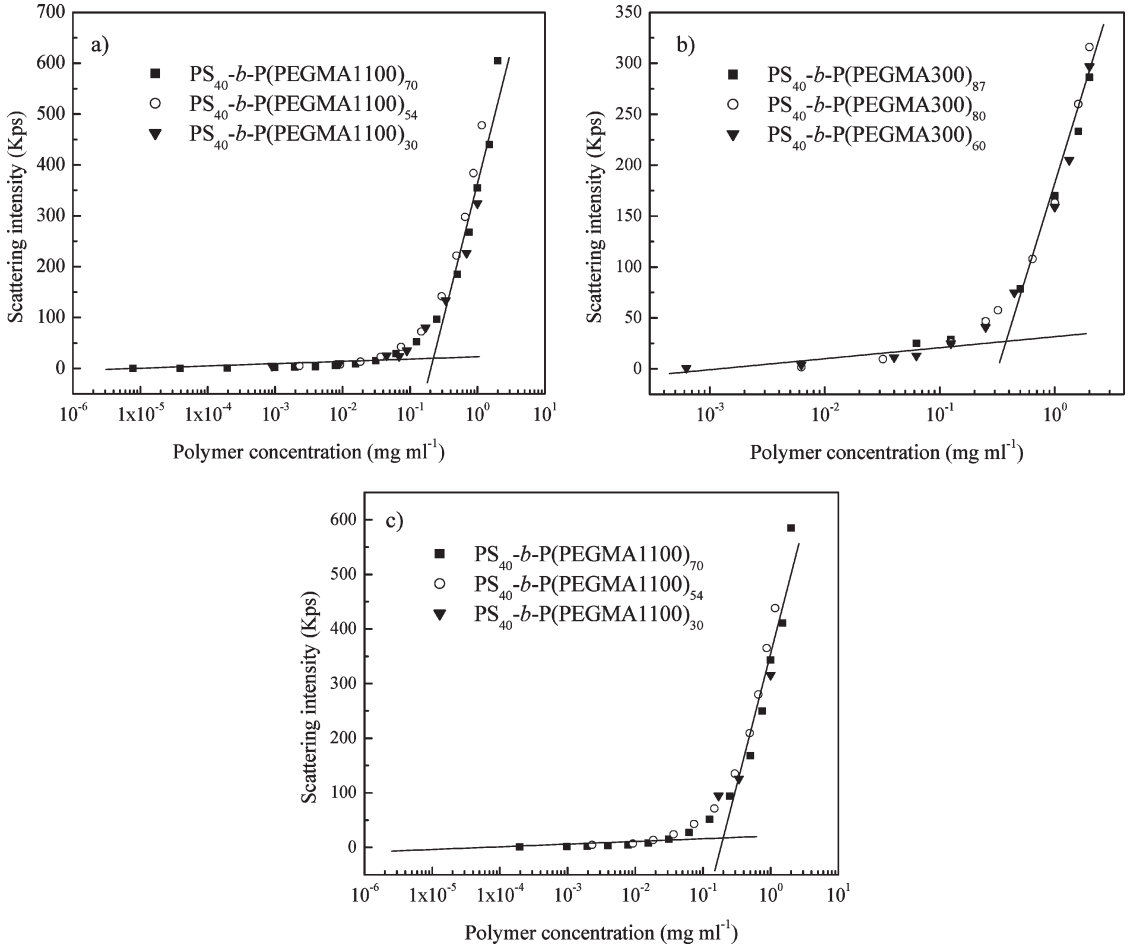

Figure 2. Scattering intensity from DLS measurements as a function of block copolymer concentration of (a) PS-*b*-P(PEGMA1100) copolymers at 25 °C, (b) PS-*b*-P(PEGMA300) copolymers at 25 °C, and (c) PS-*b*-P(PEGMA1100) copolymers at 65 °C.

Table 2. Particle Diameters (D_h) of Micelles Formed by Brush-Type Amphiphilic Block Copolymers in Aqueous Solutions (1 g L^{-1}) at 25 °C Obtained by DLS Measurements and Critical Micelle Concentrations (cmc) Obtained from Scattering Intensity Measurements as a Function of Block Copolymer Concentration at 25 and 65 °C

block copolymer	D_h (nm)	cmc (mg mL^{-1}) at 25 °C	cmc (mg mL^{-1}) at 65 °C
PS_{40}-*b*-P(PEGMA300)$_{60}$	24	0.32 ± 0.05	
PS_{40}-*b*-P(PEGMA300)$_{80}$	26	0.45 ± 0.05	
PS_{40}-*b*-P(PEGMA300)$_{87}$	36	0.46 ± 0.04	
PS_{40}-*b*-P(PEGMA1100)$_{30}$	21	0.18 ± 0.03	0.17 ± 0.03
PS_{40}-*b*-P(PEGMA1100)$_{54}$	31	0.22 ± 0.02	0.20 ± 0.02
PS_{40}-*b*-P(PEGMA1100)$_{70}$	29	0.21 ± 0.04	0.22 ± 0.02

for the PS-*b*-P(PEGMA1100) copolymers, presenting a lower tendency to form micelles.

The cmc of amphiphilic block copolymers depends on the hydrophilic/hydrophobic balance. In general, the cmc increases with increasing hydrophilicity due to the improved solubilization of the micellar structure.[33,51] On the other hand, increasing the hydrophobicity leads to a lower value of cmc. Hussain et al.[52] recently reported the self-assembly of P(PEGMA) homopolymers in aqueous solution. They concluded that the cmc depends on the length of the PEG side chain but not on the degree of polymerization, where the homopolymer with longer side chain, P(PEGMA1100), had a lower cmc. This is consistent with what has been observed in the present work, although the cmc values for all the brush-type amphiphilic block copolymers were lower than the corresponding P(PEGMA) homopolymers[52] due to the presence of the hydrophobic block of polystyrene. It has been previously reported for block copolymer systems (including linear PS-*b*-PEO) that the length of the hydrophobic block has a larger effect on the cmc than the hydrophilic chain.[53−56,32] The cmc values for each series of block copolymers with similar PEG side chain are nearly chain-length-independent, only increasing slightly with the degree of polymerization of the P(PEGMA) block. This fact can be attributed to the increase of the hydrophobic main chain as the degree of polymerization enhances, leading to only small differences on the hydrophobic/hydrophilic balance of the P(PEGMA) block.

Furthermore, the influence of temperature on the cmc was studied. Light scattering experiments were performed at 65 °C to determine the cmc of PS-*b*-P(PEGMA1100). As can be observed in Figure 2, the cmc appears to be almost independent of temperature. This unusual behavior has been previously reported for diblock copolymers of ethylene oxide and styrene oxide[57] and was attributed to the long hydrophobic block being tightly coiled in the molecular state.

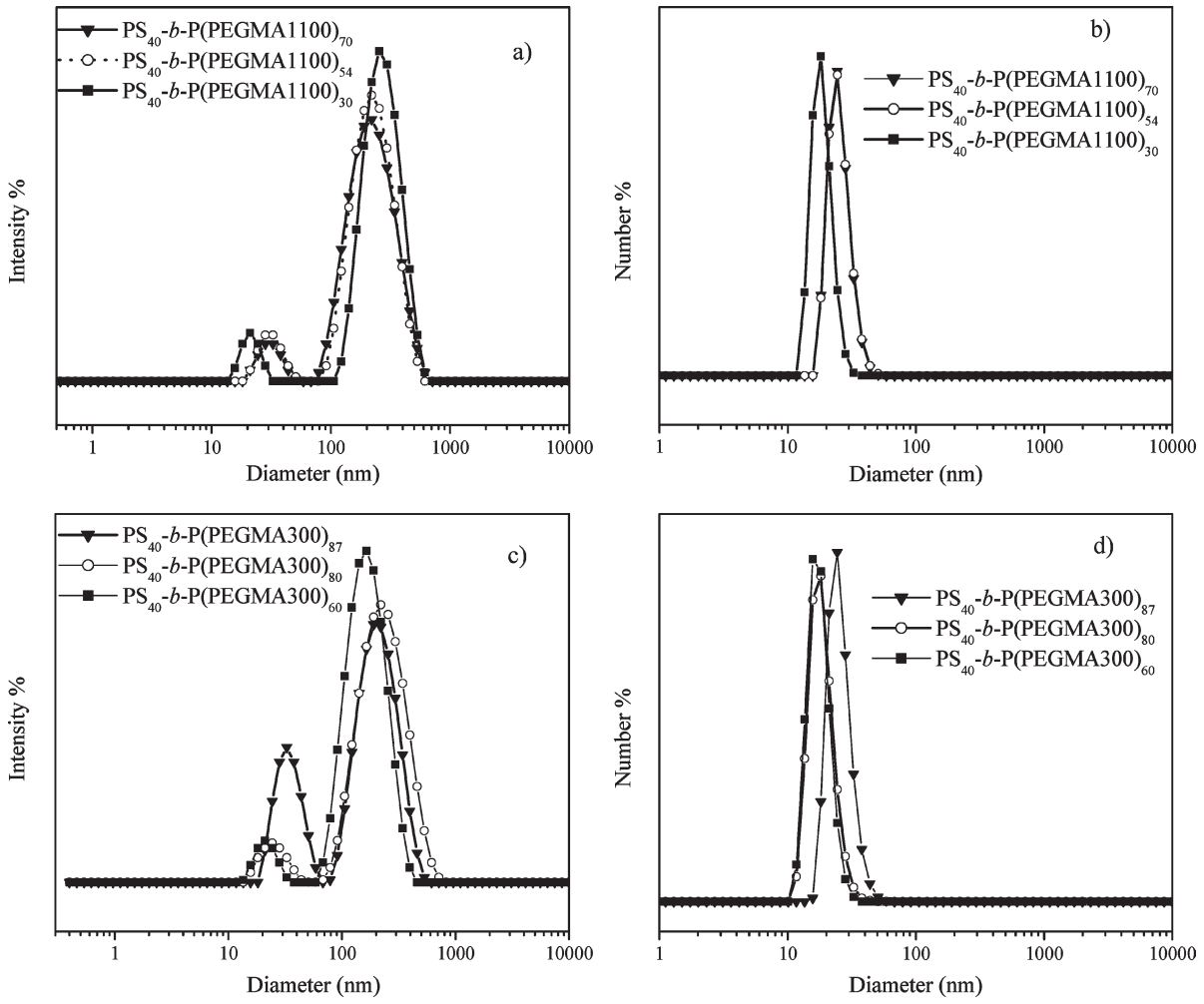

Figure 3. (a) Intensity average size distributions and (b) number-average size distributions for the copolymers PS_{40}-*b*-P(PEGMA1100)$_n$ (indicated in legend). (c) Intensity average size distributions and (d) number-average size distributions for the copolymers PS_{40}-*b*-P(PEGMA300)$_m$ (indicated in legend), determined using Malvern Dispersion Technology Software for data acquisition and analysis, applying the general purpose algorithm for calculating size distributions.

Thus, the hydrophobic interaction with water is minimized, resulting in a small positive contribution to the standard enthalpy of micellization which is balanced by a negative contribution from the dispersion interaction of the hydrophobic units in the micelle core. On the other hand, the copolymers having the shortest PEG side chain, PS-*b*-P(PEGMA300), are insoluble at 65 °C, presenting a lower critical solution temperature (LCST) or cloud point at around 60 °C. The LCST values were recorded at a copolymer concentration of 1 mg mL^{-1}, above the cmc. Above the LCST the hydrogen bonds between PEG moieties and water are broken and the copolymers become insoluble in water. As expected, the LCST slightly increases as the length of the P(PEGMA300) does, with a value of 60.3 °C for PS_{40}-*b*-P(PEGMA300)$_{60}$, 61.7 °C for PS_{40}-*b*-P(PEGMA300)$_{80}$, and 63.0 °C for PS_{40}-*b*-P(PEGMA300)$_{87}$. Moreover, the LCST values were similar to that of the P(PEGMA300) homopolymer. This type of behavior has been observed in several other studies of thermoresponsive polymers[58−61] and can be attributed to the formation of micelles which shields the hydrophobic units from the aqueous phase and decreases the effect on the cloud point. Holder et al.[32] reported that the LCSTs of PS−P(PEGMA)−PS triblock copolymer aggregates were even higher than the simple homopolymer analogues. They ascribed this result to the confined geometry at the interface of PS and P(PEGMA) chains.

The size of the micelles of both series of block copolymers was then investigated using DLS at a concentration of 1 mg mL^{-1}, which is above the cmc, at 25 °C. Figure 3 shows the intensity average particle size distribution for both series of block copolymers: PS-*b*-P(PEGMA300) and PS-*b*-P(PEGMA1100). All block copolymer solutions exhibit two distinct particle size distributions. The peaks observed around 30 nm (Table 2) are attributed to the self-assembly of the block copolymers into micelles, while the dominant peaks are ascribed to the scattering of larger aggregates. On the other hand, number-average particle size distributions displayed in Figure 3 show monomodal distributions, where the peak corresponds to the micelle formation in all the solutions; no large aggregates were observed. This observation can be explained by the higher scattering intensity of large aggregates compared to small aggregates, even at a low concentration of the larger aggregates. This conclusion is backed up by cryo-TEM measurements. Cryo-TEM images of micelles formed from PS_{40}-*b*-P(PEGMA1100)$_{70}$ block copolymers in aqueous solution are shown in Figure 4, from which it can be observed that the block copolymers mainly form micelles and just a few large aggregates, which can be attributed to the aggregation of micelles.

Large aggregates together with micelles have been observed previously in micellar aqueous solutions of block

copolymers with a glassy polystyrene core and poly(ethylene oxide) corona.[62−64] Large aggregates were interpreted as a result of the clustering of the initial spherical micelles, caused by the partial interpenetration of the poly(ethylene oxide) between micelles.[65]

Emulsion Polymerization of Styrene Using PS-*b*-P(PEGMA300) Brush-Type Block Copolymers as Stabilizers. Preparation of Hairy Particles. In order to evaluate the synthesized block copolymers as stabilizers, batch emulsion polymerizations of styrene were performed using PS-*b*-P(PEGMA300) without the addition of any cosurfactant and compared to those using SDS as a conventional surfactant. The emulsion polymerization of styrene with SDS was carried out under similar experimental conditions as employed with the polymer surfactants, i.e., 3.2 wt % of SDS and 0.8 wt % of ammonium persulfate/sodium thiosulfate at 35 °C. The emulsion polymerizations were carried out at low temperatures, 35 and 50 °C, because the copolymers are insoluble above 60 °C. The recipes for the emulsion polymerizations performed in this study are summarized in Table 3.

As shown in Figure 5, a high monomer conversion was not achieved in any of the emulsion polymerizations (entries 1−5) using the block copolymers PS-*b*-P(PEGMA300) as stabilizers.

Furthermore, from DLS and SEM analyses, it was observed that the obtained particle size distributions were quite polydisperse. The stabilization by the polymer surfactant of the latex particles was poor, and also formation of coagulum was observed at long reaction times. Piirma et al.[66] previously reported the stabilizing effectiveness of linear PS-*b*-PEO copolymers, which was found to increase as the hydrophilicity was increased. They found that the stability of the emulsion polymerization of styrene was poor when the hydrophilic/hydrophobic ratio was lower than 75 wt %, meaning a HLB value of 15. The HLB values of the block copolymers used in the present study were calculated according to the method described by Stöver et al.[48] based on the weight of the whole monomer unit (HLB_{ST}, Table 1). Using this method, all of the copolymers present a HLB values higher than 16 and should allow the stabilization of styrene in water emulsion. However, because of the hydrophobic main chain of the P(PEGMA), the HLB values are probably better determined taking into account only the PEG side chain (Table 1), now yielding HLB values below 11.5. These HLB_{MOD} values were calculated as follows:

$$HLB_{MOD} = 20\left(\frac{nM_{EO}x}{M_{n,NMR}}\right)$$

where n is the degree of polymerization of the P(PEGMA) block, M_{EO} is the molecular weight of one ethylene oxide

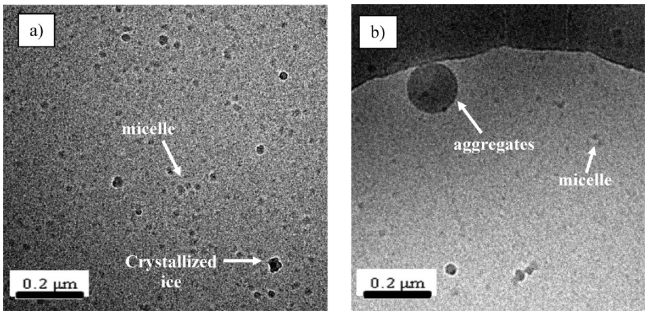

Figure 4. Cryo-TEM images of (a) the micelles formed from PS_{40}-*b*-$P(PEGMA1100)_{70}$ block copolymers and (b) large aggregates also present in the sample, embedded in vitreous ice. The observed dark particles correspond to tiny ice crystals.

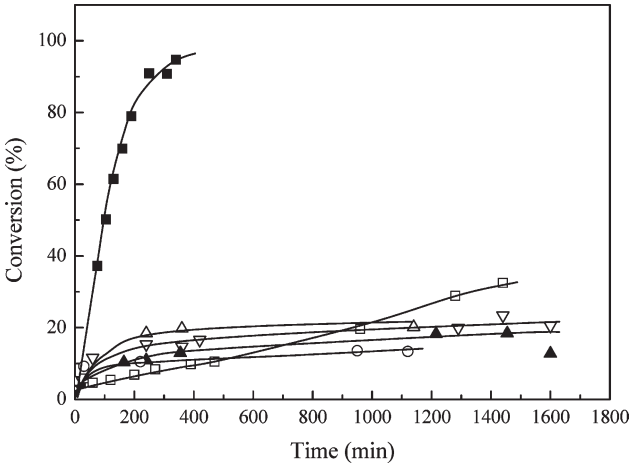

Figure 5. Evolution of monomer conversion with time for the emulsion polymerization of styrene using a redox initiator system ammonium persulfate/sodium thiosulphate (0.8 wt %) and PS-*b*-P(PEGMA300) block copolymers as stabilizers: (■) 3.2 wt % of SDS as surfactant at 35 °C (entry 13), (○) 3.2 wt % of PS_{40}-*b*-$P(PEGMA300)_{60}$ at 35 °C (entry 1), (▲) 3.2 wt % of PS_{40}-*b*-$P(PEGMA300)_{80}$ at 35 °C (entry 2), (▽) 3.2 wt % of PS_{40}-*b*-$P(PEGMA300)_{87}$ at 35 °C (entry 3), (△) 5.7 wt % of PS_{40}-*b*-$P(PEGMA300)_{87}$ at 35 °C (entry 4), (□) 3.2 wt % of PS_{40}-*b*-$P(PEGMA300)_{87}$ at 50 °C (entry 5).

Table 3. Synthesis Conditions Used for the Preparation of Polystyrene Latexes via Emulsion Polymerization Using Redox Initiator System Ammonium Persulfate/Sodium Thiosulfate and PS-*b*-P(PEGMA) Block Copolymers as Stabilizers

entry no.	surfactant	styrene (wt %)	surfactant (wt %) (based on the monomer)	initiator[a] (wt %) (based on the monomer)	T (°C)
1	PS_{40}-*b*-$P(PEGMA300)_{60}$	16.6	3.2	0.8	35
2	PS_{40}-*b*-$P(PEGMA300)_{80}$	16.6	3.2	0.8	35
3	PS_{40}-*b*-$P(PEGMA300)_{87}$	16.6	3.2	0.8	35
4	PS_{40}-*b*-$P(PEGMA300)_{87}$	16.6	5.7	0.8	35
5	PS_{40}-*b*-$P(PEGMA300)_{87}$	16.6	3.2	0.8	50
6	PS_{40}-*b*-$P(PEGMA1100)_{30}$	16.6	3.2	0.8	35
7	PS_{40}-*b*-$P(PEGMA1100)_{54}$	16.6	3.2	0.8	35
8	PS_{40}-*b*-$P(PEGMA1100)_{70}$	16.6	3.2	0.8	35
9	PS_{40}-*b*-$P(PEGMA1100)_{70}$	16.6	1.6	0.8	35
10	PS_{40}-*b*-$P(PEGMA1100)_{30}$	16.6	3.2	0.8	70
11	PS_{40}-*b*-$P(PEGMA1100)_{54}$	16.6	3.2	0.8	70
12	PS_{40}-*b*-$P(PEGMA1100)_{70}$	16.6	3.2	0.8	70
13	SDS	16.6	3.2	0.8	35
14	SDS	16.6	3.2	0.8	70

[a] Redox initiator system 0.8 wt % of ammonium persulfate and 0.8 wt % sodium thiosulfate was employed in the polymerizations at 35 °C. Sodium thiosulphate was added continuously during the reaction. Potassium persulfate (0.8 wt %) was used in the polymerization carried out at 70 °C.

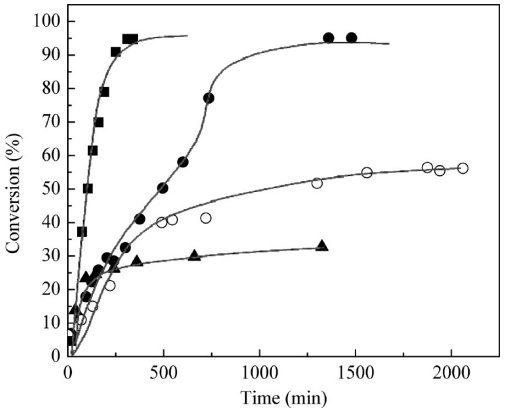

Figure 6. Emulsion polymerization of styrene at 35 °C using a redox initiator system, 0.8 wt % of ammonium persulfate/sodium thiosulphate and 3.2 wt % of surfactants: (■) SDS, (▲) PS_{40}-*b*-$P(PEGMA1100)_{30}$ (entry 6), (○) PS_{40}-*b*-$P(PEGMA1100)_{54}$, (entry 7), (●) PS_{40}-*b*-$P(PEGMA1100)_{70}$ (entry 8).

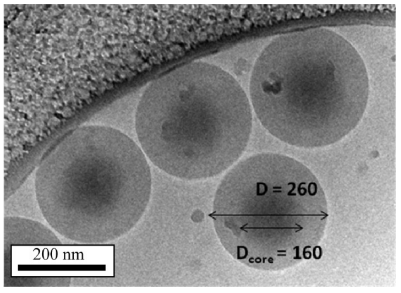

Figure 7. Cryo-TEM image of a polystyrene latex obtained via emulsion polymerization of styrene at 35 °C using 3.2 wt % of PS_{40}-*b*-$P(PEGMA1100)_{70}$ as surfactant.

unit (44 g mol^{-1}), x is the number of ethylene oxide units of the side chain (x = 4.5 for the PS_{40}-*b*-P(PEGMA300) and x = 22.7 for the PS_{40}-*b*-P(PEGMA1100)), and $M_{n,NMR}$ is the molecular weight of the block copolymer calculated by NMR.

These block copolymers, with short poly(ethylene glycol) side chain, did not efficiently stabilize the emulsion of styrene, even though they were water-soluble at 35 °C (and considering a decrease in the LCST due to the salting-out effect of the monomer). The poor colloidal stability can be probably attributed to the retarded molecular diffusion of the block copolymers from the surfaces of the monomer droplets and micelles.

Emulsion Polymerization of Styrene Using PS-*b*-P(PEGMA1100) Brush-Type Block Copolymers as Stabilizers. Preparation of Hairy Particles. Next, the emulsion polymerization of styrene was carried out using the synthesized PS-*b*-P(PEGMA1100) block copolymers under the same experimental conditions as above, 35 °C and redox initiator systems (see Table 3, entries 6−8). Figure 6 shows the conversion−time profiles for emulsion polymerization of styrene using PS-*b*-P(PEGMA1100) block copolymers. It is clear that the increase in hydrophilicity, and therefore mobility in the heterogeneous reaction system, improves the efficiency of the surfactant, and higher conversions were obtained compared with those using the PS-*b*-P(PEGMA300) copolymers. Still, high monomer conversions were only obtained using the block copolymer with the longest hydrophilic block, i.e., PS_{40}-*b*-$P(PEGMA1100)_{70}$. The presence of the rate increase at higher conversion in the emulsion polymerization using PS_{40}-*b*-$P(PEGMA1100)_{70}$ may be related to the gel effect. The monomer concentration in the latex particles decreases as the polymerization advances, increasing the viscosity inside the particles. Therefore, the bimolecular termination rate decreases causing an accumulation of radicals within the particles which leads in turn to an increase of the rate of polymerization, R_p. When comparing the rate of polymerization using these nonionic block copolymer surfactants to that of the emulsion polymerization employing a conventional surfactant, SDS, under the same experimental conditions, we observe that it is slower. This is probably caused by the fact that the number of particles, N_p, is lower and the presence of a thick interfacial layer which can act as a barrier for radical entry, depressing the rate of polymerization.[67,68]

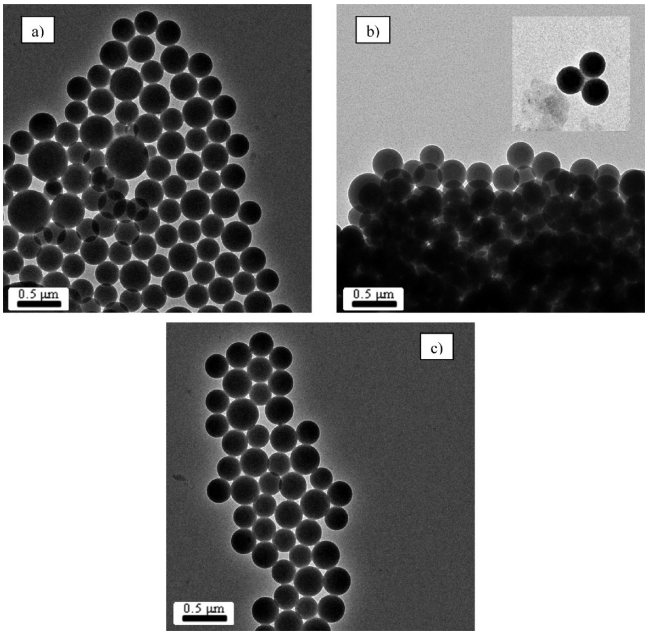

Figure 8. TEM images of polystyrene latexes obtained via emulsion polymerization of styrene at 35 °C using 3.2 wt % of copolymer surfactant: (a) PS_{40}-*b*-$P(PEGMA1100)_{30}$, (b) PS_{40}-*b*-$P(PEGMA1100)_{54}$, and (c) PS_{40}-*b*-$P(PEGMA1100)_{70}$.

The efficiency of the PS-*b*-P(PEGMA1100) copolymers as stabilizers was also evaluated through analysis of the particle size distribution of the final latex particles. Cryo-TEM (Figure 7) shows the corresponding colloidal particles stabilized by PS_{40}-*b*-$P(PEGMA1100)_{70}$ to be spherical and the distribution to be very monodisperse. More interesting, those particles present a core−shell structure with a dark core representing the polystyrene surrounded by a dense and homogeneous layer of P(PEGMA).

The transmission electron micrographs of all final polystyrene particles are shown in Figure 8. As also reported in Table 4, monodisperse particles with a diameter of 286 nm (from TEM) were obtained using the PS_{40}-*b*-$P(PEGMA1100)_{70}$ block copolymer. Latex particles stabilized by PS_{40}-*b*-$P(PEGMA1100)_{30}$ and PS_{40}-*b*-$P(PEGMA1100)_{54}$ are not as monodisperse as those stabilized by PS_{40}-*b*-$P(PEGMA1100)_{70}$, and also larger particles are observed. Moreover, residual monomer inside the particles was observed in the later cases due to the limited conversion achieved.

Figure 9 shows SEM images of polystyrene particles prepared with PS_{40}-*b*-$P(PEGMA1100)_{54}$ and PS_{40}-*b*-$P(PEGMA1100)_{70}$. Few larger particles were observed in the SEM image of the sample with PS_{40}-*b*-$P(PEGMA1100)_{54}$ as stabilizer. The monodisperse polystyrene particles stabilized by PS_{40}-*b*-$P(PEGMA1100)_{70}$ were capable of self-assembly

Table 4. Particle Sizes and Polydispersities Determined by DLS Measurements (D_{DLS} and PDI_{DLS}) and by TEM (D_{TEM} and PDI_{TEM}) of the Polystyrene Latex Stabilized with 3.2 wt % of PS_{40}-*b*-P(PEGMA1100) Copolymers Obtained by Emulsion Polymerization of Styrene at 35 and 70 °C

block copolymer	T (°C)	D_{DLS}[b] (nm)	PDI_{DLS}[b]	D_{TEM}[c] (nm)	PDI_{TEM}[c]
PS_{40}-*b*-P(PEGMA1100)$_{30}$	35	405	0.15	217	1.3
PS_{40}-*b*-P(PEGMA1100)$_{54}$	35	461	0.09	323	1.1
PS_{40}-*b*-P(PEGMA1100)$_{70}$	35	367	0.08	286	1.1
PS_{40}-*b*-P(PEGMA1100)$_{70}$[a]	35	564	0.03	494	1.1
PS_{40}-*b*-P(PEGMA1100)$_{30}$	70	816	0.22	328	2.1
PS_{40}-*b*-P(PEGMA1100)$_{54}$	70	1647	0.23	260	3.3
PS_{40}-*b*-P(PEGMA1100)$_{70}$	70	1231	0.27	377	3.4

[a] Particles stabilized with 1.6 wt % of PS_{40}-*b*-P(PEGMA1100)$_{70}$. [b] Obtained from DLS using Malvern Dispersion Technology Software for data acquisition and analysis, applying the general purpose algorithm for calculating size distributions. [c] Determined from TEM using the software ImageJ. PDI_{TEM} were calculated according to $PDI = D_w/D_n$, where D_w is the weight-average diameter, $D_w = \sum n_i D_i^4 / \sum n_i D_i^3$, and D_n is the number-average diameter, $D_n = \sum n_i D_i / n_i$ (n_i is the number of particles with diameter D_i).

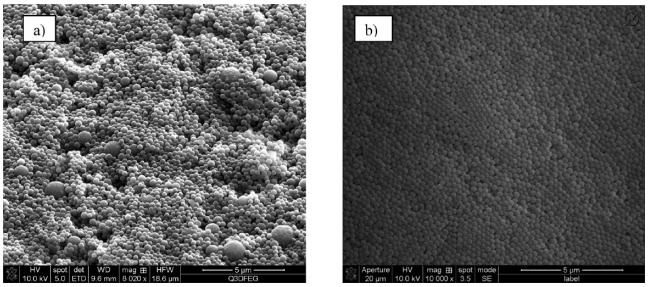

Figure 9. SEM images of polystyrene latex prepared via emulsion polymerization of styrene at 35 °C with 3.2 wt % of block copolymer stabilizers: (a) PS_{40}-*b*-P(PEGMA1100)$_{54}$ and (b) PS_{40}-*b*-P(PEGMA1100)$_{70}$ block copolymers.

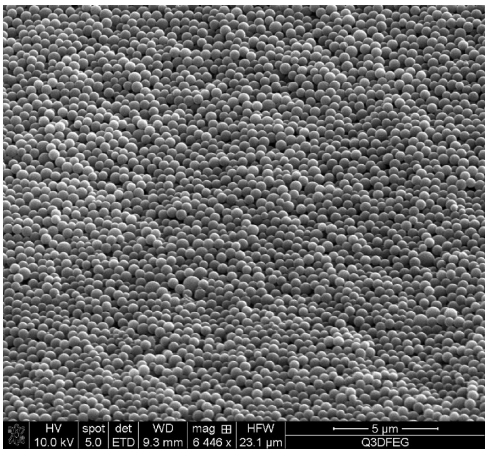

Figure 10. SEM image of the polystyrene latex prepared via emulsion polymerization of styrene at 35 °C with 1.6 wt % PS_{40}-*b*-P(PEGMA1100)$_{70}$ block copolymer.

from their dispersion and formed relatively close packed ordered arrays or colloidal crystals, exhibiting a pink coloration.

The effect of polymeric surfactant concentration was also studied. The emulsion polymerization was carried out under the same experimental conditions, using 1.6 wt % of PS_{40}-*b*-P(PEGMA1100)$_{70}$ (entry 9). The particles are still quite monodisperse as can be seen in Figure 10. Figure 11 shows the conversion vs reaction time for the emulsion polymerization using different concentrations of block copolymer surfactant.

The rate of polymerization decreases when the concentration of block copolymer is reduced. Besides, a gel effect was observed. This was studied by examining the molecular weight distribution of both polystyrene latexes with 1.6 and 3.2 wt %, which present similar molecular weights,

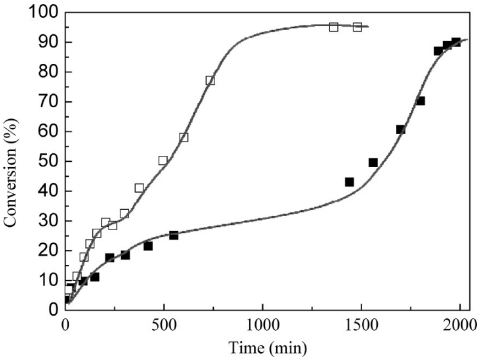

Figure 11. Conversion vs time for emulsion polymerization of styrene at 35 °C using 0.8 wt % of ammonium persulfate/sodium thiosulphate and various amounts of PS_{40}-*b*-P(PEGMA1100)$_{70}$: (□) 3.2 wt % and (■) 1.6 wt %.

$M_n = 304 \times 10^3$ g mol^{-1} ($M_w/M_n = 2.65$) and $M_n = 306 \times 10^3$ g mol^{-1} ($M_w/M_n = 2.58$), respectively, although the number of particles varies. The emulsion polymerization of styrene using 1.6 wt % of PS_{40}-*b*-P(PEGMA1100)$_{70}$ leads to larger particles with diameters of 494 nm (determined by TEM) and number of particles, $N_p = 2.5 \times 10^{15}$ L_{latex}^{-1}, while the particles obtained with 3.2 wt % of copolymers present diameters of 286 nm and $N_p = 1.3 \times 10^{16}$ L_{latex}^{-1}. Considering this large difference in particle numbers, we would have expected a difference in M_n. We cannot think of any obvious reason why this is not the case, other than that a gel effect is observed, which may change the termination kinetics.

The average particle diameters measured by dynamic light scattering for these two latexes are 564 nm (PDI = 0.03) and 367 nm (PDI = 0.08) for the surfactant concentrations of 1.6 and 3.2 wt %, respectively (see Table 4). The observation that the diameters obtained by TEM are smaller than those from DLS can be explained by the fact that DLS leads to the hydrodynamic radius including the solvated layer of P(PEGMA), whereas in TEM measurements this layer is collapsed.

Another important parameter in the sterically stabilized emulsion polymerization is the temperature. Increasing the temperature may greatly reduce hydrogen bonding between poly(ethylene oxide) and water, even though the block copolymers having P(PEGMA1100) are soluble in water in the whole temperature range and do not have a cloud point. In order to investigate the influence of the polymerization temperature, the emulsion reactions of styrene using PS-*b*-P(PEGMA1100) copolymers were also performed at 70 °C (Table 3, entries 10−12). As illustrated in Figure 12, the rate of polymerization at 70 °C is much higher for all the emulsifiers as compared to the emulsion polymerization

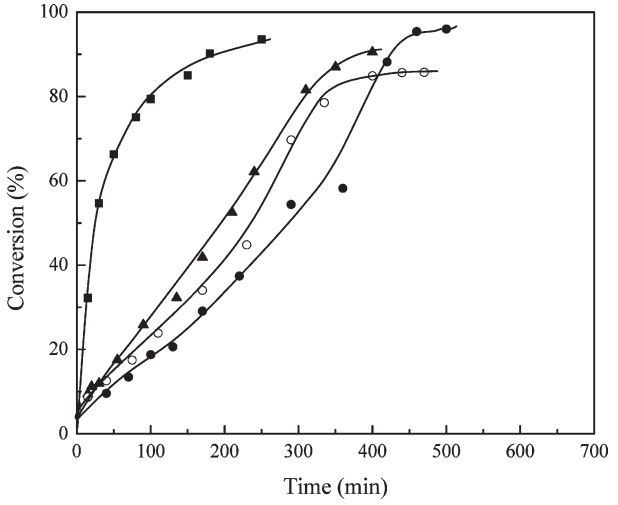

Figure 12. Emulsion polymerization of styrene at 70 °C using 0.8 wt % of potassium persulfate as thermal initiator and 3.2 wt % of surfactants: (■) SDS, (●) PS_{40}-*b*-$P(PEGMA1100)_{70}$, (○) PS_{40}-*b*-$P(PEGMA1100)_{54}$, (▲) PS_{40}-*b*-$P(PEGMA1100)_{30}$.

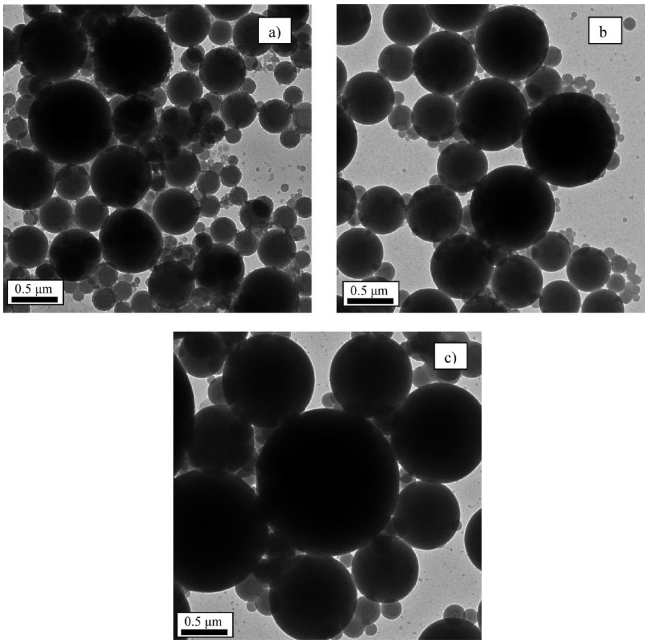

Figure 13. TEM images of polystyrene latexes obtained via emulsion polymerization of styrene at 70 °C using 0.8 wt % of potassium persulfate as thermal initiator and 3.2 wt % of surfactants: (a) PS_{40}-*b*-$P(PEGMA1100)_{30}$, (b) PS_{40}-*b*-$P(PEGMA1100)_{54}$, and (c) PS_{40}-*b*-$P(PEGMA1100)_{70}$.

performed at 35 °C. Also, the limiting conversion increases considerably. In general, the rate of polymerization increases for higher temperatures because both the initiation and propagation rates increase significantly. Furthermore, in sterically stabilized emulsion polymerization, the contraction of the poly(ethylene glycol) chains with increasing temperature is accompanied by a decrease in the thickness of the interfacial layer, which can increase the radical entry rate coefficient.[68]

In contrast to the situation at 35 °C, all obtained polystyrene latices present a very broad particle size distribution, as displayed in TEM images (Figure 13) and as listed in Table 4. As discussed previously, the cmc is not much affected by the temperature. Nevertheless at higher temperature, the hydrophilicity of the emulsifiers is lower and most of the nonionic surfactants initially dissolved in the aqueous phase partition toward the styrene,[69] despite the fact that the block copolymers are still water-soluble at that temperature. As a result, the concentration of surfactant in the aqueous phase is reduced (it may even become lower than the cmc), and therefore also the number of micelles will be reduced. Under those conditions, homogeneous nucleation can operate and the surfactant can be continuously released from the monomer droplets to the aqueous phase. Consequently, polydisperse particle size distributions are obtained at high temperature with PS-*b*-P(PEGMA1100) brush-type block copolymers.

Table 5. Static (θ_S), Advancing (θ_A), and Receding (θ_A) Contact Angles (deg) of Water Obtained by Needle−Syringe on Film Samples after Annealing at 130 °C for 24 h

film	θ_S	θ_A	θ_R
PS latex with SDBS	92.5	109 ± 0.9	77.6 ± 1.0
PS latex with PS_{40}-*b*-$P(PEGMA1100)_{70}$ (1.6 wt %)	80.6	92.4 ± 0.4	54.3 ± 0.3
PS latex with PS_{40}-*b*-$P(PEGMA1100)_{70}$ (3.2 wt %)	77.7	88.2 ± 0.4	58.1 ± 1.2

The above results indicate that the block copolymer with the longest block length, containing the longest PEG side chain, PS_{40}-*b*-$P(PEGMA1100)_{70}$, is the most effective stabilizer, leading to monodisperse particles and good colloidal stability at low polymerization temperature. These hairy particles, containing different amounts of PS_{40}-*b*-$P(PEGMA1100)_{70}$, 3.2 and 1.6 wt %, were employed in the preparation of antifouling films (see following section).

Antifouling Properties of Polymer Films Obtained from the Synthesized Hairy Particles. Polymer films were prepared from the synthesized polystyrene particles functionalized with P(PEGMA) in order to investigate their resistance to protein adsorption. The films were prepared on aluminum plates, dried, and annealed at 130 °C for 24 h to obtain flat surfaces. A film from a polystyrene latex stabilized by a conventional surfactant, 4-dodecylbenzenesulfonic acid (SDBS), was also prepared as a control experiment. First, contact angle measurements were performed to study the hydrophilic properties of the polystyrene films, which reflect the presence of the copolymer surfactant at the interface. Static, θ_S, advancing, θ_A (highest stable angle observed when the drop volume is increased), and receding, θ_R (lowest stable angle observed when the drop volume is decreased), contact angles were measured and shown in Table 5. The films prepared from the hairy latex particles containing the surfactant PS_{40}-*b*-$P(PEGMA1100)_{70}$ display significantly lower contact angles than those containing SDBS due to the presence of the block copolymer surfactants. An increase in block copolymer concentration leads to a further decrease in contact angle. Upon the annealing at 130 °C in dry air, the surfactants tend to migrate toward the air/polymer interface; however, the high annealing temperature under dry conditions enables chain conformation changes and orientation of the hydrophobic tail at the interface.[70,71] Concerning the block copolymer surfactants with P(PEGMA) segments, despite their hydrophilicity, the unfolding of the P(PEGMA) is reduced due to the end-group effects caused by the high amount of methyl terminal groups. The side chains of P(PEGMA) are oriented toward the surface, exposing the methyl termini to the surface.[72,73] The significant differences in the contact angle between advancing and receding values, hysteresis, can be explained by the mobility and reorientation of the surface polymeric chains.[72,74−76]

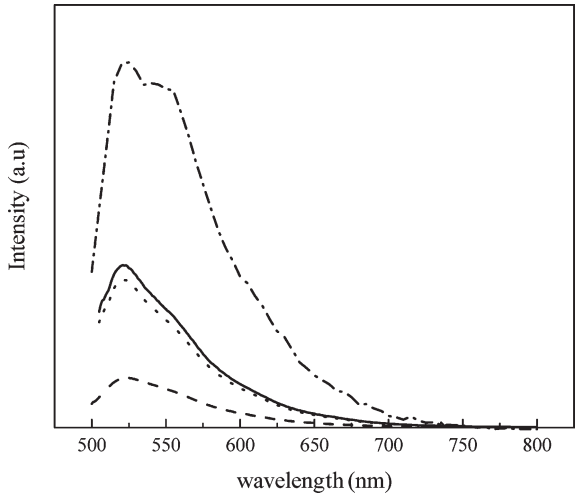

Figure 14. Emission spectra at 490 nm excitation wavelength of polystyrene films formed from latexes with (− · −) SDBS, (· · ·) 1.6 wt % of PS_{40}-*b*-P(PEGMA1100)$_{70}$, (—) 1.6 wt % of PS_{40}-*b*-P(PEGMA1100)$_{70}$ annealed, and (---) 3.2 wt % of PS_{40}-*b*-P(PEGMA1100)$_{70}$.

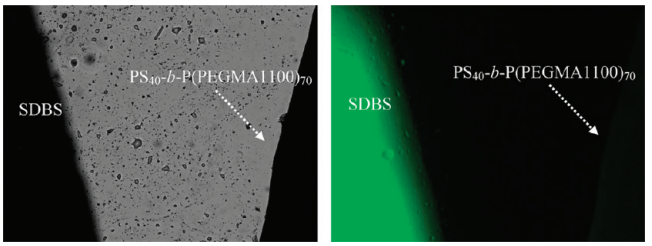

Figure 15. (a) Optical microscopy and (b) fluorescence microscopy images of films formed from polystyrene latexes with PS_{40}-*b*-P(PEGMA1100)$_{70}$ (1.6 wt %) and SDBS.

Once it was established that the polymer surface is enriched in PEG moieties, the antifouling or protein-resistant properties of these films were studied. Annealed and nonannealed films, prepared from hairy particles with 1.6 or 3.2 wt % PS_{40}-*b*-P(PEGMA1100)$_{70}$, and a film prepared from a polystyrene latex stabilized with SDBS were immersed in phosphate buffered saline solution (PBS, pH = 7.4) at room temperature containing 1 mg mL^{-1} of bovine albumin−fluorescein isothiocyanate conjugate (BSA−FITC). After incubation for 24 h, the films were washed sequentially with excess PBS and distilled water. The relative fluorescence intensity, which was taken as a measure for the amount of adsorbed protein, was determined by steady-state fluorescence spectroscopy, as illustrated in Figure 14. The intensity of the wavelength of maximum emission is much higher in the case of the surface containing the conventional surfactant than that on films containing PS_{40}-*b*-P(PEGMA1100)$_{70}$ copolymers, meaning more nonspecific adsorption of BSA−FITC. Moreover, the appearance of a shoulder at longer wavelength can be observed. Probably, the presence of two peak maxima is caused by hydrophobic interactions together with electrostatic interactions between BSA and the SDBS surfactant.[77,78] In the emission spectra of the films containing PS_{40}-*b*-P(PEGMA1100)$_{70}$, only a small peak appears at 521 nm which corresponds to slight hydrophobic interactions. The amount of adsorbed protein increases as the concentration of block copolymer surfactant decreases, and it is higher in annealed films. This observation is due to the reorientation of the block copolymer upon annealing, which provides a more hydrophobic surface and thus more adsorption of proteins.

The antifouling properties of P(PEGMA) were also illustrated using fluorescence microscopy. As shown in Figure 15, almost no fluorescence can be detected from the films containing PS_{40}-*b*-P(PEGMA1100)$_{70}$ (1.6 wt %), in contrast to those prepared from the SDBS-stabilized latex.

Conclusions

Brush-type amphiphilic diblock copolymers based on polystyrene and two different nonionic comblike hydrophilic blocks, P(PEGMA300) and P(PEGMA1100), were synthesized via ATRP in a controlled manner. All the block copolymers form spherical micelles with diameters of around 30 nm and also large aggregates. The cmc of the PS_{40}-*b*-P(PEGMA1100)$_n$ copolymers was ∼2 times lower than that found for the PS_{40}-*b*-P(PEGMA300)$_m$ polymers, but the value is hardly affected by the length of the hydrophilic block (*n* and *m*, respectively) for each series of block copolymers. Thus, we can conclude that the cmc depends mainly on the length of the PEG side chain but not much on the degree of polymerization of the P(PEGMA) block (at least for the investigated chain lengths). None of the PS_{40}-*b*-P(PEGMA300)$_m$ copolymers act as an efficient stabilizer in the emulsion polymerization of styrene, irrespective of the length of the P(PEGMA300) segment (in the studied molecular weight range). However, increasing the length of PEG side chain, in this study from PEGMA300 to PEGMA1100, improves the performance of the block copolymers as stabilizers, with increasing performance for longer hydrophilic block lengths. These results suggest that the surfactant behavior of comblike P(PEGMA) segments is different from that of the corresponding linear PEG because of the influence of the hydrophobic main chain. Monodisperse hairy particles with core−shell structure were obtained in the polymerization of styrene at 35 °C using the copolymer with the longest P(PEGMA1100) chain, PS_{40}-*b*-P(PEGMA1100)$_{70}$. At higher polymerization temperatures, probably caused by the fact that the PS_{40}-*b*-P(PEGMA1100)$_n$ copolymer is partially soluble in the monomer droplets, no monodisperse latices were obtained. Finally, the preparation of polystyrene films from the synthesized hairy particles, containing the brush-type copolymers, can effectively suppress nonspecific protein adsorption.

Acknowledgment. This work was financially supported by the Foundation Emulsion Polymerization (SEP). A. Muñoz-Bonilla gratefully acknowledges MICINN-CSIC for her postdoctoral grant. We also thank Syed Imran Ali, Hector Tello Manon, Rinske Knoop, Monique Mballa, and Mark Berix for the SEM and (cryo)-TEM analysis.

References and Notes

(1) Kumacheva, E.; Kalinina, O.; Lilge, L. *Adv. Mater.* **1999**, *11*, 231–234.
(2) Pham, H. H.; Gourevich, I.; Oh, J. K.; Jonkman, J. E.; Kumacheva, E. *Adv. Mater.* **2004**, *16*, 516–520.
(3) Xu, X.; Asher, S. A. *J. Am. Chem. Soc.* **2004**, *126*, 7940–7945.
(4) Kawaguchi, H. *Prog. Polym. Sci.* **2000**, *25*, 1171–1210.
(5) Li, D. J.; Sheng, X.; Zhao, B. *J. Am. Chem. Soc.* **2005**, *127*, 6248–6256.
(6) Min, K.; Hu, J.; Wang, C.; Elaissari, A. *J. Polym. Sci., Part A: Polym. Chem.* **2002**, *40*, 892–900.
(7) D'Agosto, F.; Charreyre, M.-T.; Pichot, C.; Gilbert, R. G. *J. Polym. Sci., Part A: Polym. Chem.* **2003**, *41*, 1188–1195.
(8) Riess, G.; Labbe, C. *Macromol. Rapid Commun.* **2004**, *25*, 401–435.
(9) Burguiere, C.; Chassenieux, C.; Charleux, B. *Polymer* **2003**, *44*, 509–518.
(10) Save, M.; Manguian, M.; Chassenieux, C.; Charleux, B. *Macromolecules* **2005**, *38*, 280–289.
(11) Burguiere, C.; Pascual, S.; Bui, C.; Vairon, J.-P.; Charleux, B.; Davis, K. A.; Matyjaszewski, K.; Betremieux, I. *Macromolecules* **2001**, *34*, 4439–4450.

(12) Liu, S.; Armes, S. P. *Angew. Chem., Int. Ed.* **2001**, *41*, 1413–1416.
(13) Stoffelbach, F.; Belardi, B.; Santos, J. M. R. C. A.; Tessier, L.; Matyjaszewski, K.; Charleux, B. *Macromolecules* **2007**, *40*, 8813–8816.
(14) Otsuka, H.; Nagasaki, Y.; Kataoka, K. *Curr. Opin. Colloid Interface Sci.* **2001**, *6*, 3–10.
(15) Nakayama, Y.; Miyamura, M.; Hirano, Y.; Goto, K.; Matsuda, T. *Biomaterials* **1999**, *20*, 963–970.
(16) Jo, S.; Park, K. *Biomaterials* **2000**, *21*, 605–616.
(17) Tugulu, S.; Klok, H.-A. *Biomacromolecules* **2008**, *9*, 906–912.
(18) Corey, J. M.; Wheeler, B. C.; Brewer, G. J. *J. Neurosci. Res.* **1991**, *30*, 300–307.
(19) Brink, C.; Osterberg, E.; Holmberg, K.; Tiberg, F. *Colloids Surf., A* **1992**, *66*, 149–156.
(20) Patrucco, E.; Ouasti, S.; Vo, C. C.; Leonardis, P. D.; Pollicino, A.; Armes, S. P.; Scandola, M.; Tirelli, N. *Biomacromolecules* **2009**, *10*, 3130–3140.
(21) Kingshott, P.; Thissen, H.; Griesser, H. J. *Biomaterials* **2002**, *23*, 2043–2056.
(22) Kizhakkedathu, J. N.; Janzen, J.; Le, Y.; Kainthan, R. K.; Brooks, D. E. *Langmuir* **2009**, *25*, 3794–3801.
(23) Hyun, J.; Ma, H.; Zhang, Z.; Beebe, T. P.; Chilkoti, A. *Adv. Mater.* **2003**, *15*, 576–579.
(24) Brown, A. A.; Khan, N. S.; Steinbock, L.; Huck, W. T. S. *Eur. Polym. J.* **2005**, *41*, 1757–1765.
(25) Popescu, D. C.; Lems, R.; Rossi, N. A. A.; Yeoh, C. T.; Loss, J.; Holder, S. J.; Bouten, C. V. C.; Sommerdijk, N. A. J. M. *Adv. Mater.* **2005**, *17*, 2324–2329.
(26) Lee, B. S.; Chi, Y. S.; Lee, K. B.; Kim, Y. G.; Choi, I. S. *Biomacromolecules* **2007**, *8*, 3922–3929.
(27) Zhang, L.; Eisenberg, A. *Science* **1995**, *268*, 1728–1745.
(28) Xu, R.; Winnik, M. A.; Riess, G.; Chu, B.; Croucher, M. D. *Macromolecules* **1992**, *25*, 644–652.
(29) Förster, S.; Plantenberg, T. *Angew. Chem., Int. Ed.* **2002**, *41*, 689–714.
(30) Bes, L.; Angot, S.; Limer, A.; Haddleton, D. M. *Macromolecules* **2003**, *36*, 2493–2499.
(31) Cheng, Z.; Zhu, X.; Kang, E. T.; Neoh, K. G. *Langmuir* **2005**, *21*, 7180–7185.
(32) Holder, S. J.; Durand, G. G.; Yeoh, C.-T.; Illi, E.; Hardy, N. J.; Richardson, T. H. *J. Polym. Sci., Part A: Polym. Chem.* **2008**, *46*, 7739–7756.
(33) Tan, B. H.; Hussain, H.; Liu, Y.; He, C. B.; Davis, T. P. *Langmuir*, DOI: 10.1021/la902816b.
(34) Robinson, K. L.; de Paz-Banez, M. V.; Wang, X. S.; Armes, S. P. *Macromolecules* **2001**, *34*, 5799–5805.
(35) Holder, S. J.; Rossi, N. A. A.; Yeoh, C. T.; Durand, G. G.; Boerakker, M. J.; Sommerdijk, N. A. J. M. *J. Mater. Chem.* **2003**, *13*, 2771–2778.
(36) Street, G.; Illsley, D.; Holder, S. J. *J. Polym. Sci., Part A: Polym. Chem.* **2005**, *43*, 1129–1143.
(37) Rao, J. Y.; Xu, J.; Luo, S. Z.; Liu, S. Y. *Langmuir* **2007**, *23*, 11857–11865.
(38) Liu, H.; Jiang, X. Z.; Fan, J.; Wang, G. H.; Lui, S. Y. *Macromolecules* **2007**, *40*, 9074–9083.
(39) Park, C. W.; Lee, S. J.; Kim, D.; Lee, D. S.; Kim, S. C. *J. Polym. Sci., Part A: Polym. Chem.* **2008**, *46*, 1954–1963.
(40) Sheibat-Othman, N.; Bourgeat-Lami, E. *Langmuir* **2009**, *25*, 10121–10133.
(41) Ho, B. S.; Tan, B. H.; Tan, J. P. K.; Tam, K. C. *Langmuir* **2008**, *24*, 7698–7703.
(42) Dupin, D.; Howse, J. R.; Armes, S. P.; Randall, D. P. *J. Mater. Chem.* **2008**, *18*, 545–552.
(43) Pich, A.; Lu, Y.; Adler, H.-J. *Colloid Polym. Sci.* **2003**, *281*, 907–915.
(44) Dupin, D.; Fujii, S.; Armes, S. P. *Langmuir* **2006**, *22*, 3381–3387.
(45) Chern, C. -S.; Lee, C. *J. Polym. Sci., Part A: Polym. Chem.* **2002**, *40*, 1608–1624.
(46) Fournier, D.; Hoogenboom, R.; Thijs, H. M. L.; Paulus, R. M.; Schubert, U. S. *Macromolecules* **2007**, *40*, 915–920.
(47) Bergenudd, H.; Coullerez, G.; Jonsson, M.; Malmström, E. *Macromolecules* **2009**, *42*, 3302–3308.
(48) Ali, M. M.; Stöver, H. D. H. *Macromolecules* **2004**, *37*, 5219–5227.
(49) Zhang, L.; Barlow, R. J.; Eisenberg, A. *Macromolecules* **1995**, *28*, 6055–6066.
(50) Jada, A.; Hurtrez, G.; Siffert, B.; Riess, G. *Macromol. Chem. Phys.* **1996**, *197*, 3697–3710.
(51) Zamurovic, M.; Christodoulou, S.; Vazaios, A.; Iatrou, E.; Pitsialis, M.; Hadjichristidis, N. *Macromolecules* **2007**, *40*, 5835–5849.
(52) Hussain, H.; Mya, K. Y.; He, C. *Langmuir* **2008**, *24*, 13279–13286.
(53) Gao, Z.; Eisenberg, A. *Macromolecules* **1993**, *26*, 7353–7360.
(54) Riess, G. *Prog. Polym. Sci.* **2003**, *28*, 1107–1170.
(55) Booth, C.; Attwood, D. *Macromol. Rapid Commun.* **2000**, *21*, 501–527.
(56) Calderara, F.; Hruska, Z.; Hurtrez, G.; Lerch, J. P.; Nugay, T.; Riess, G. *Macromolecules* **1994**, *27*, 1210–1215.
(57) Kelarakis, A.; Havredaki, V.; Rekatas, C. J.; Booth, C. *Phys. Chem. Chem. Phys.* **2001**, *3*, 5550–5552.
(58) Patrickios, C. S.; Forder, C.; Armes, S. P.; Billingham, N. C. *J. Polym. Sci., Part A: Polym. Chem.* **1996**, *34*, 1529–1541.
(59) Ringsdorf, H.; Venzmer, J.; Winnik, F. M. *Macromolecules* **1991**, *24*, 1678–1686.
(60) Chung, J. E.; Yokoyama, M.; Suzuki, K.; Aoyagi, T.; Sakurai, Y.; Okano, T. *Colloids Surf., B* **1997**, *9*, 37–48.
(61) Chung, J. E.; Yokoyama, M.; Aoyagi, T.; Sakurai, Y.; Okano, T. *J. Controlled Release* **1998**, *53*, 119–130.
(62) Xu, R.; Winnik, M. A.; Riess, G.; Chu, B.; Croucher, M. D. *Macromolecules* **1992**, *25*, 644–652.
(63) Mortensen, K.; Brown, W.; Almdal, K.; Alami, E.; Jada, A. *Langmuir* **1997**, *13*, 3635–3645.
(64) Bronstein, L. M.; Chernyshov, D. M.; Timofeeva, G. I.; Dubrovina, L. V.; Valetsky, P. M.; Khokhlov, A. R. *Langmuir* **1999**, *15*, 6195–6200.
(65) Lombardo, D.; Micali, N.; Villari, V.; Kiselev, M. A. *Phys. Rev. E* **2004**, *70*, 021402.
(66) Jialanella, G. L.; Firer, E. M.; Piirma, I. *J. Polym. Sci., Part A: Polym. Chem.* **1992**, *30*, 1925–1933.
(67) Capek, I.; Chudej, J.; Janickova, S. *J. Polym. Sci., Part A: Polym. Chem.* **2003**, *41*, 804–820.
(68) Capek, I. *Adv. Colloid Interface Sci.* **2002**, *99*, 77–162.
(69) Okudo, M.; Kobayashi, H.; Matoba, T.; Oshima, Y. *Langmuir* **2006**, *22*, 8727–8731.
(70) Shin, J.-S.; Lee, D.-Y.; Ho, C.-G.; Kim, J.-H. *Langmuir* **2000**, *16*, 1882–1888.
(71) Iyengar, D. R.; Perutz, S. M.; Dai, C.-A.; Ober, C. K.; Kramer, E. J. *Macromolecules* **1996**, *29*, 1229–1234.
(72) Yokoyama, H.; Miyamae, T.; Han, S.; Ishizone, T.; Tanaka, K.; Takahara, A.; Torikai, N. *Macromolecules* **2005**, *38*, 5180–5189.
(73) Muñoz-Bonilla, A.; Ibarboure, E.; Papon, E.; Rodriguez-Hernandez *J. Polym. Sci., Part A: Polym. Chem.* **2009**, *47*, 2262–2271.
(74) Muller, P.; Sudre, G.; Theodoly, O. *Langmuir* **2008**, *24*, 9541–9550.
(75) Tavana, H.; Jehnichen, D.; Grundke, K.; Hair, M. L.; Neumann, A. W. *Adv. Colloid Interface Sci.* **2007**, *134*−*135*, 236–248.
(76) Van Damme, H. S.; Hogt, A. H.; Feijen, J. *J. Colloid Interface Sci.* **1986**, *114*, 167–172.
(77) Chakraborty, T.; Chakraborty, I.; Moulik, S. P.; Ghosh, S. *Langmuir* **2009**, *25*, 3062–3074.
(78) Park, J. M.; Muhoberac, B. B.; Dubin, P. L.; Xia, J. *Macromolecules* **1992**, *25*, 290–295.